IEEE Access
Multidisciplinary | Rapid Review | Open Access Journal

Received October 27, 2020, accepted November 7, 2020, date of publication November 10, 2020,
date of current version November 23, 2020.

Digital Object Identifier 10.1109/ACCESS.2020.3037176

Pitch Effect of Helical Coils of Electromagnetic Forming

WENTING ZHANG[1,2], HANG ZHOU[1,2], XIAOGUANG LIANG[3], XIANQI SONG[1,2], LIJUN ZHOU[1,2], SHUIXIANG LI[4], MENG YANG[1,2], AND XINHUI ZHU[1,2]

[1]College of Electrical Engineering and New Energy, China Three Gorges University, Yichang 443002, China
[2]Hubei Provincial Engineering Technology Research Center for Power Transmission Line, China Three Gorges University, Yichang 443002, China
[3]Beijing Institute of Aerospace Systems Engineering, Beijing 100076, China
[4]College of Urban and Environment Science, Central China Normal University, Wuhan 430079, China

Corresponding authors: Xinhui Zhu (540022126@qq.com) and Meng Yang (1397047121@qq.com)

This work was supported by National Natural Science Foundation of China (No. 51707104), the State Scholarship Fund of China (No. 201908420196).

ABSTRACT At present, solenoid (helical) coils are widely used in various researches, especially electromagnetic forming (EMF), due to their advantages of simple manufacture and high magnetic field strength. However, in the study of EMF, there are still some defects in the high precision calculation of solenoid coils in the magnetic field the main reason is that the solenoid coil is of non-axisymmetric structure, which is generally equivalent to the 2-D or 3-D axisymmetric structure in practical research. Not only can it ignore the effect of the pitch effect of the solenoid coil, but also causes a certain deviation in the calculation of the magnetic field. Hence, this paper establishes 5 helical coils and 3-D axisymmetric finite element coils models with different layers for comparative analysis. The simulation results show that the magnetic flux density distribution deviation of helical coil and the 3-D axisymmetric coil is small and can be ignored when the coil layers are 1 or 2 layers. However, the number of linear circles increasing, the deviation between the two increases obviously. Therefore, in the study of EMF, the effect of solenoid coil pitch effect on magnetic field calculation can be ignored when the layers, radius and pitch of helical coils are used less whereas the effect of solenoid coil pitch effect on magnetic field calculation must be considered when the layers, radius and pitch of helical coils are used more.

INDEX TERMS Pitch effect, helical coil, numerical simulation, electromagnetic forming.

I. INTRODUCTION

Solenoid coils have been widely used in various researches due to their advantages of simple manufacture and high magnetic field strength, such as permanent magnet machines [1], [2], electronic transformers [3], medical implants [4], fluid dynamics [5], [6] and Electromagnetic forming (EMF) [7]–[9]. Especially in the study of EMF, it mainly includes four parts: solenoid coil, workpiece, mold, and the external circuit. The solenoid coil is mainly used as a driving coil and energy conversion medium, which generates a pulsed magnetic field and eddy current on the workpiece, and then drives the workpiece to form. Thus, the importance of solenoid coil is self-evident [10], [11].

The associate editor coordinating the review of this manuscript and approving it for publication was Xiaodong Liang.

The EMF research is mainly through simulations and experiments. However, with its complexity in experimental equipment and difficulty in building an experimental platform, researchers often need to rely on the simulations to form the process, proving its feasibility under the premise of environmental protection and energy-saving. Nevertheless, due to the non-axisymmetric structure of the helical coil, it is very difficult to establish the actual helical coil model, which eventually leads to a sharp increase in the high precision calculation of the magnetic field, and the simulation results cannot converge. Hence, researchers usually use software such as COMSOL [12]–[14], ANSYS/MEGA [15], [16] and LS-DYNA [17], [18] to analyze the magnetic field by equating the solenoid coil model with a 2-D or 3-D axisymmetric model. What's more, these studies mainly focus on aspects such as electromagnetic bulging [19], [20], electromagnetic

welding [21], [22], electromagnetic superposed forming [23], and the electromagnetic-assisted forming [24], [25].

Moreover, as shown in Fig.1, the winding process of the solenoid coil is generally carried out in a helical manner, and the coil will appear a misalignment of the width of the coil. Also, as shown in Fig.2, when the solenoid coil is a multi-layer and multi-turn structure, the dislocation and gap of layer change will occur. As a result, the solenoid coil has a pitch effect in the calculation of the magnetic field, which makes it difficult to solve the high-precision calculation of the magnetic field. So, this process of equivalent simplification inevitably brings some deviations to the simulation of magnetic field. Therefore, in the study of EMF, although the 2-D or 3-D axisymmetric equivalent model of solenoid coil reduces the calculation amount and makes it easy to solve, the influence of the non-axisymmetric structure of solenoid coil on the magnetic field generated by it is ignored.

FIGURE 1. Schematic diagram of the helical coil model.

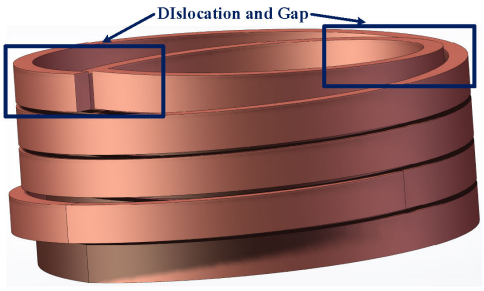

FIGURE 2. The dislocation and gap of the helical coil when changing layers and turns.

Thereby, to solve these problems, this paper adopts SOLIDWORKS drawing software to build 5 actual helical coil models with different layers and analyzes the reasons for the difference of winding coils in engineering practice from the perspective of principle. Consequently, when the same voltage excitation is applied by the finite element software, the magnetic field of the helical coil structure is analyzed and compared with the simulation results of the 3-D axisymmetric coil model. The simulation results show that the magnetic flux density distribution deviation of helical coils and 3-D axisymmetric coils is small and can be ignored when the number of linear coils is 1 or 2 layers. However, as the number of linear circles increases, the deviation between the two increases significantly. Accordingly, in the study of EMF, when the number of layers of solenoid coils is small, the effect of its pitch effect can be ignored; on the contrary, when the number of layers of the solenoid coil is large, the effect of the pitch effect must be considered when calculating the magnetic field.

II. THEORY

The difference between the helical winding mode of the forming coil and the symmetric model mainly comes from three aspects: the winding angle (slope), the interlaminar transition between the coil layers and the coil outgoing mode. Since EMF involves the coupling process of transient multiple physical fields, so the current simulation methods are mainly included loose coupling, sequential coupling, and full coupling.

A. THE INTERLAMINAR TRANSITION AND THE OUTGOING MODE

As shown in Fig.2, when the coil is multi-layer and multi-turn, the coil in the transition between the layers, the coil needs to be wound from one layer to another layer. The winding radius of the wire will increase from the previous layer to the next layer in a range, resulting in an irregular ''transition gap'' in this range, which leads to the coil in the flange area appear uneven effect, and thereby affecting the configuration distribution of the magnetic field.

Besides, the helical coil is located in a high voltage and high current environment in EMF, so the selection of the outgoing position of the coil in the winding process is not in the same position, especially for the coil winding on the same side. Common outgoing positions include opposite outgoing, quarter outgoing etc., to ensure good insulation performance when the coil is loaded and discharged.

B. THE WINDING ANGLE

Further, according to the right-hand rule, the long straight wire with current only has a circumferential magnetic field. Therefore, in this paper, the finite element method is used to analyze the axisymmetric coil as a ''long straight wire'', and it can be seen that the axisymmetric coil only has circular current $\overrightarrow{I_{phi}}$ thus producing uniform magnetic field distribution. However, the current simulation model is shown in Fig.3, and the helical coil is equivalent to the 2-D or 3-D axisymmetric model in the simulation modeling. In other words, the current simulation analysis of the simplified helical coil model ignores the influence of the current component of the coil axial excitation. In practical engineering operation, the radial magnetic field generated will seriously affect the strength of the axial magnetic field and may occur singularity, thus affecting the distribution of the magnetic field. Therefore, the current value $\overrightarrow{I_c}$ of the current value in the symmetric and helical coils can be decomposed into:

$$\begin{cases} \textbf{\textit{Symmetric}} : \overrightarrow{\boldsymbol{I}_c} = \overrightarrow{\boldsymbol{I}_{phi}} \\ \textbf{\textit{Helical}} : \overrightarrow{\boldsymbol{I}_c} = \overrightarrow{\boldsymbol{I}_{phi}} + \overrightarrow{\boldsymbol{I}_z} \end{cases} \tag{1}$$

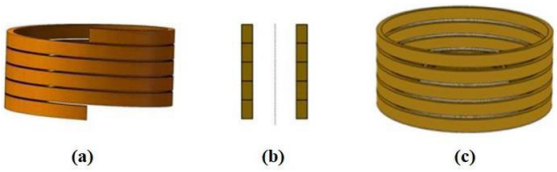

FIGURE 3. The axisymmetric equivalent treatment of helical coils; (a) helical coil, (b) simplified 2-D symmetric coil, (c) simplified 3-D symmetric coil.

C. THE FULL COUPLING SIMULATION METHOD

Under the fully coupled model including circuit, electromagnetic field, and solid mechanical field, the geometric displacement and forming speed of the workpiece were comprehensively considered to further improve the calculation accuracy [26]–[28]. Besides, compared with loose coupling and sequential coupling, the fully coupled model has the highest computational accuracy [29].

Therefore, the fully-coupled model was used in this paper. When the initial circuit parameters of the system are determined, the discharge current through the forming coil, the magnetic force acting on the workpiece, and the plastic deformation of the workpiece can be calculated. The procedure is executed as follows:

a): The discharge current flowing through the coil can be calculated by the ''Global ODEs and DAEs'' model (Eq.2).

$$\begin{cases} \overrightarrow{U_0} - \dfrac{1}{C_0}\displaystyle\int_0^t \overrightarrow{I_c}\,dt = \overrightarrow{Uc} \\ R_w\overrightarrow{I_w} + \dfrac{dL_w\overrightarrow{I_w}}{dt} + \dfrac{dM\overrightarrow{I_c}}{dt} = 0 \\ \dfrac{dL_c\overrightarrow{I_c}}{dt} + \dfrac{dM\overrightarrow{I_w}}{dt} = Vp \\ (R_0 + R_c)\,\overrightarrow{I_c} + L_0\dfrac{\mathrm{d}\overrightarrow{I_c}}{dt} + \left(\dfrac{dL_c\overrightarrow{I_c}}{dt} + \dfrac{dM\overrightarrow{I_w}}{dt}\right) = \overrightarrow{Uc} \end{cases} \tag{2}$$

where C_0, $\overrightarrow{Uc}$ R_0, L_0 are respectively the capacitor value, the capacitor voltage (the capacitor is charged by the DC device [29]), the resistance, and the inductance of the connecting circuit lines. $\overrightarrow{I_c}$ is the coil current, $\overrightarrow{I_w}$ is the eddy current induced in the workpiece, R_c is the resistance of the coil, Lc is the equivalent inductance of the coil, V_p is the dynamic electrodynamic potential, and M is the mutual inductance between the coil and the workpiece.

b): The eddy current and field distribution can be calculated by solving the magnetic vector potential equations in the ''magnetic fields'' model (Eq.3), which uses the current density of the coil, obtained from Eq.2. It should be noted that the currents flowing through the coils are assumed to be evenly distributed.

$$\begin{cases} \nabla \times \boldsymbol{H} = \boldsymbol{J} \\ \nabla \times \boldsymbol{E} = -\dfrac{d\boldsymbol{B}}{dt} \\ \nabla \cdot \boldsymbol{B} = \boldsymbol{0} \\ \boldsymbol{J} = \delta_e \boldsymbol{E} \end{cases} \tag{3}$$

where $\boldsymbol{H}$ is the magnetic intensity, $\boldsymbol{J}$ is the current density, $\boldsymbol{B}$ is the magnetic flux density, E is the electric intensity, and σ_e is the electrical conductivity.

c): The deformation of the workpiece can be calculated by solving the structural field model in the ''Solid Mechanics'' model (Eq.4), which uses magnetic force density, obtained from Eq.4, as a body force imparted on the workpiece. The calculated workpiece velocity is added to Eq.3 with the magnetic field to reflect the effect of the motional electromotive force on the electromagnetic equations (Eq.5).

$$\overrightarrow{J} \times \overrightarrow{B} = \overrightarrow{f} = \rho\frac{\partial^2 u}{\partial^2} - \nabla \cdot \delta \tag{4}$$

$$\nabla \times \boldsymbol{E} = -\frac{\partial B\left(r\left(t\right), z\left(t\right), t\right)}{\partial t} + \nabla \times \left(V \times B\left(r\left(t\right), z\left(t\right), t\right)\right) \tag{5}$$

The value of $\boldsymbol{V_p}$ will change with the workpiece deformation due to the variation of mutual inductance between the coil and the workpiece. Furthermore, a new induced potential $\boldsymbol{V_p}$ of the coil should be calculated and then the calculation returns to step 1 until the discharge comes to an end. In the simulation, to avoid the meshes distort for large deformation, a ''Moving Mesh'' model is taken to update the shapes of mesh elements with the deformation of the workpiece based on an arbitrary Lagrangian-Eulerian method.

Moreover, due to the current in the coil is pulse current, so the magnetic flux density $\boldsymbol{B}$ can be also expressed as:

$$\overrightarrow{B} = \alpha\left(d\overrightarrow{I_c}/dt\right) \tag{6}$$

where α is the proportionality coefficient. Therefore, combining Eq.1 and Eq.6, it can be known that when the excitation is consistent, the magnetic induction intensity $\overrightarrow{B_{helical}}$ generated by the helical coil can be expressed as:

$$\overrightarrow{B_{helical}} = \alpha\frac{d\left(\overrightarrow{I_{phi}} + \overrightarrow{I_z}\right)}{dt} \tag{7}$$

Therefore, the magnetic field generated by the helical coil is different from the equivalent symmetric model, which affects the distribution and strength of the magnetic field.

III. MODEL

To better verify the simplified equivalent 2-D and 3-D axisymmetric solenoid models, the magnetic field simulation deviation and the helical coil pitch effect can be ignored. The 3-D symmetric (equivalent to 2-D axisymmetric) and 3-D helical coil models were established for comparative analysis.

Besides, the grid of the simulation model in this paper uses the physical field control grid method to construct a network of given cell size. As shown in Figure 4, to research the effect of mesh accuracy on the calculation results, in the process of establishing the simulation model, four groups of mesh method of different sizes were divided, and their serial numbers were 1, 2, 3, and 4. The maximum unit setting of the coil part is 0.3mm, 0.4mm, 0.5mm, 0.6mm respectively.

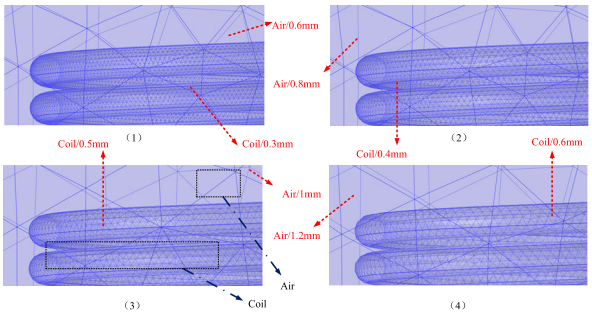

FIGURE 4. Different precision grid division methods.

The maximum cell setting of the outer air field of the coil is 0.6mm, 0.8mm, 1.0mm, 1.2mm.

As shown in Table 1, the calculation deviation of the magnetic flux density between the 3-D helical coil and the 2-D symmetric model does not exceed 3% in the model calculation by establishing the network with different accuracy. Due to the 3D model's sensitivity to the degree of mesh division, not only the amount of calculation will increase, but the simulation results will also be difficult to converge if the division is too low. Therefore, the meshing method adopted in this paper can meet the calculation requirements.

TABLE 1. Model calculation results of different meshing method.

Meshing method	3-D helical magnetic flux	Symmetric magnetic flux	Deviation
1	3.98T	4.07T	2.2%
2	3.98T	4.08T	2.4%
3	3.99T	4.08T	2.2%
4	4.07T	4.08T	0.2%

A. ONE LAYER OF HELICAL ADN 3-D SYMMETRIC COIL MODEL

Furthermore, for Case 1: (a) the coil consists of 5 turns in each layer, with a spacing of 0.5 mm between the turns and the spacing between the layers. The coil is made of copper wire with a cross-section of $\pi \times 0.52$ mm^2. The specific model is shown in Fig.4, and their main parameters were in Table 1. (b) during the transition between layers, the ''transition gap'' of the coil is within a quarter of the circumference. (c) coil outgoing mainly discusses the unilateral outgoing mode, and the default position of both outgoing lines is the same axial direction, which is not discussed in this paper.

B. MULTULAYER HELICAL AND 3-D SYMMETRIC COIL MODEL

On the other hand, the specific models are shown in Table 2, and the input current used and the geometry of the coil in Case 2 is the same as that in Case 1. In this paper, the helical coil and 3-D symmetric coil models with 5 different layers

TABLE 2. Main parameters for Case 1.

Coil	3-D helical		3-D symmetric	
Inner diameter of the coil	20 mm	20 mm	Symbol	Value
Outer diameter of the coil	24 mm	24 mm	U_f	6.8 kV
Height of the coil	12 mm	12 mm	C_f	120 μF
Radius of the wire	1 mm	1 mm	R_f	8 mΩ
Distance between turns	0.5 mm	0.5 mm	L_f	10 μH
Distance between layers	0.5 mm	0.5 mm	R_{df}	8 mΩ

(each layer is 5 turns) as shown in Case 2 are also established. They are defined as L1-L5 (helical coil), D1-D5 (3-D axisymmetric coil), in which L1 and D1 are 5 turns in the first layer, L2 and D2 are 10 turns in the second layer, L3 and D3 are 15 turns in the third layer, L4 and D4 are 20 turns in the fourth layer, and L5 and D5 are 25 turns in the fifth layer. (3) Geometric parameters of the sheet metal: the workpiece used is an A1060–O with a diameter of 70 mm and the sheet metal thickness is 1 mm.

IV. SIMULATION RESULTS AND DISCUSSION

A. THE SIMULATION RESULTS OF CASE 1 AND CASE 2

The distribution of the magnetic flux density at the below of the coil in different layers is shown in Fig.5. It can be seen that the maximum magnetic flux density of the helical coil is 3.96 T, and the maximum magnetic flux density of the 3-D axisymmetric coil is 3.93 T. The flux density deviation in these two models is small, only 0.03 T, and within acceptable limits in different turns.

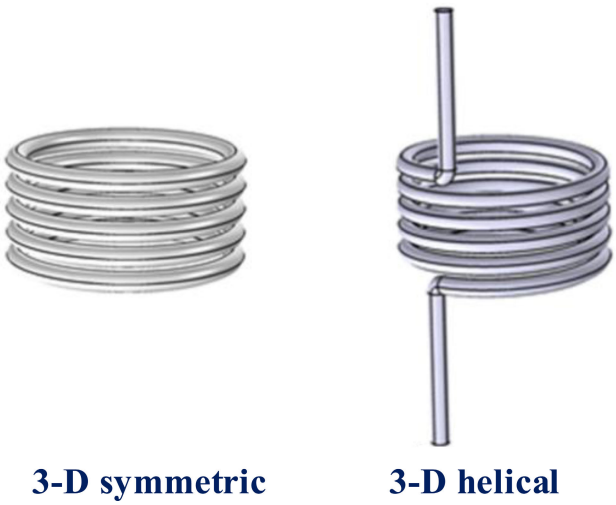

FIGURE 5. The schematic diagram of two models.

In addition, when the coil has only one layer, the magnetic field distribution is shown in Fig.6. It can be seen that the magnetic field distribution at the center of the z-axis of the coil and 15 mm away from the center is basically the same, except that there is a slight offset in the axial direction.

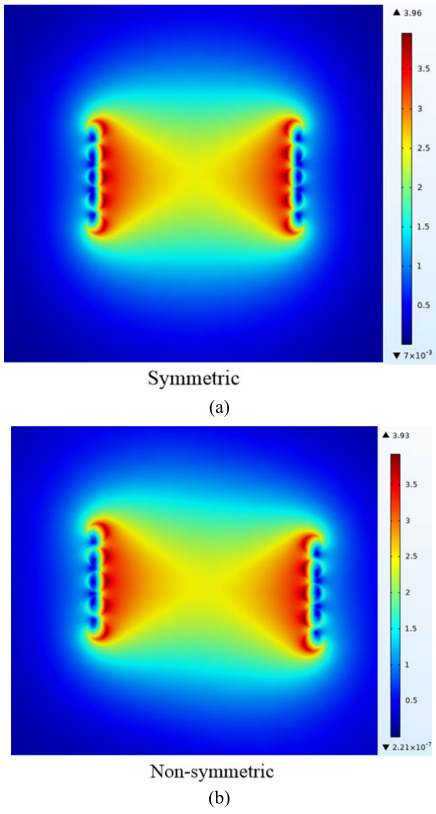

FIGURE 6. The distribution of the magnetic flux density; (a) 3-D axisymmetric coil, (b) helical coil.

B. THE SIMULATION RESULTS OF CASE 2

The distribution of the magnetic flux density at the below of the coil in different layers is shown in Fig.7. It can be seen from Fig.7, with the increase of the number of layers of the coil, the distribution of the magnetic field generated by the coil will be different. Besides, when the coils are 1 or 2 layers, the magnetic flux density distribution of solenoid coils is basically the same as that of the 3-D axisymmetric coil model. Therefore, after the solenoid coils are equivalent (the 3-D axisymmetric model), the coil pitch effect can be ignored. However, when the number of layers of the linear circle increases, the deviation of the magnetic flux density distribution of the two models increases obviously. Therefore, the effect of the solenoid coil on the pitch effect must be considered when calculating the magnetic field.

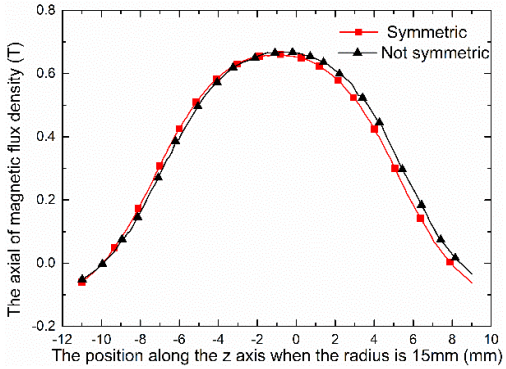

FIGURE 7. The distribution of the axial magnetic flux density.

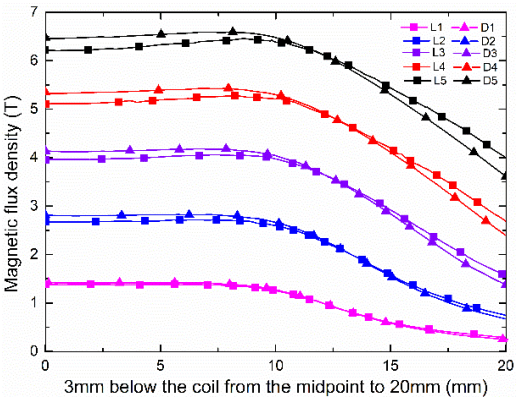

FIGURE 8. The distribution of the magnetic flux density at the below of the coil in different layers.

C. THE SIMULATION RESULTS OF DIFFERENT PITCH AND RADIUS

Fig. 9 (a) shows the distribution of the magnetic flux density under the coil with a radius of 8 mm and 10 mm when the pitch is 0.5 mm. It can be seen that when the coil radius is 8mm, the maximum magnetic flux density of the spiral coil is 4.2T, the maximum magnetic flux density of the 2-D axisymmetric model coil is 4.28T, and the error accuracy of the two is about 1.8%. When the coil radius is 10mm, the maximum magnetic flux density of the spiral coil is 4.08T, the maximum magnetic flux density of the 2-D axisymmetric model coil is 3.95T, and the error accuracy of the two is about 3.1%.

Fig. 9 (b) shows the distribution of the magnetic flux density under the coil with a radius of 8 mm and 10 mm when the pitch is 1 mm. It can be seen that when the coil radius is 8mm, the maximum magnetic flux density of the spiral coil is 3.89T, the maximum magnetic flux density of the 2-D axisymmetric model coil is 3.97T, and the error accuracy of the two is about 2%. When the coil radius is 10mm, the maximum magnetic flux density of the spiral coil is 3.68T, the maximum magnetic flux density of the 2-D axisymmetric model coil is 3.79T, and the error accuracy of the two is about2.9%.

Fig. 9 (c) shows the distribution of the magnetic flux density under the coil with a radius of 8 mm and 10 mm when the pitch is 1.5 mm. It can be seen that when the coil radius is 8mm, the maximum magnetic flux density of the spiral coil is 3.67T, the maximum magnetic flux density of the 2-D axisymmetric model coil is 3.79T, and the error accuracy of the two is about 3.1%. When the coil radius is 10mm, the maximum magnetic flux density of the spiral coil is 3.48T, the maximum magnetic flux density of the 2-D axisymmetric model coil is 3.59T, and the error accuracy of the two is about 3%.

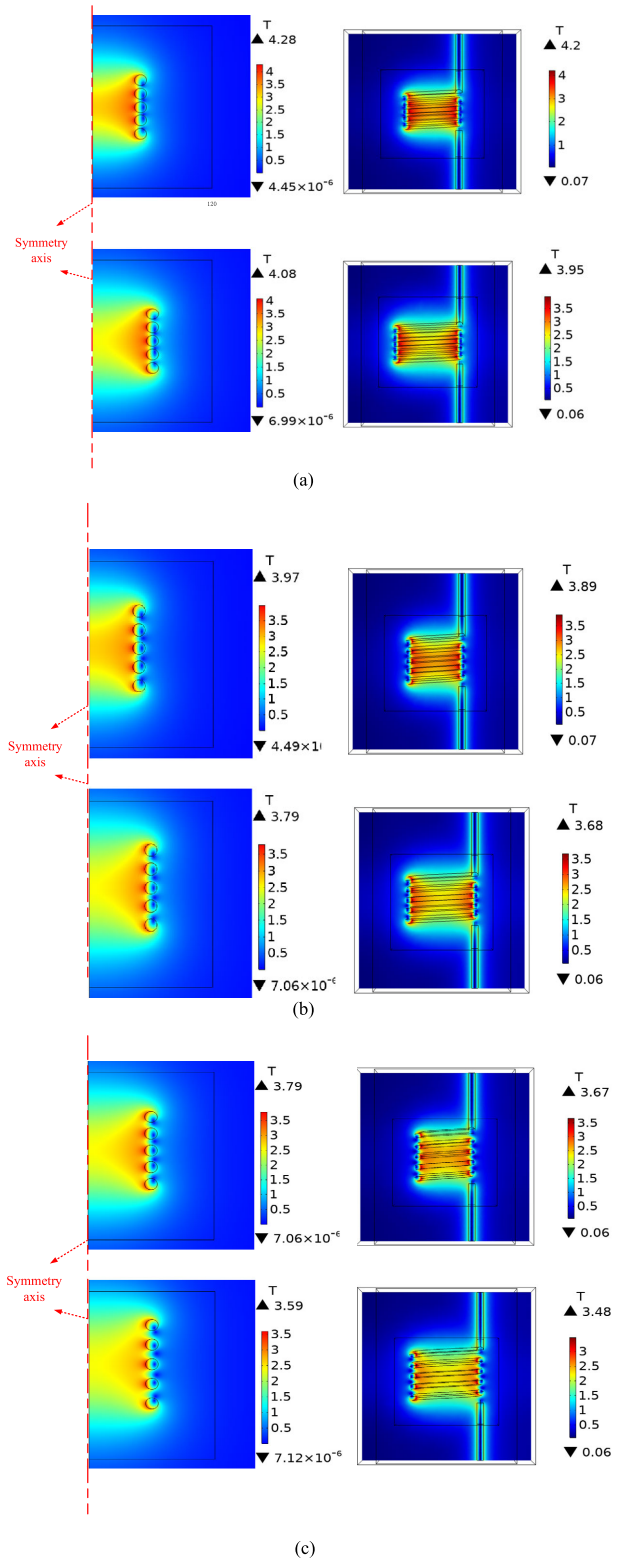

FIGURE 9. The distribution of the magnetic flux density in 2-D model and 3-D model under different pitch and radius. (a) pitch is 0.4mm, (b) pitch is 0.5mm, (c) pitch is 0.6mm.

Through Table 3, the influence of coil pitch and radius on the magnetic flux density of the coil can be seen more clearly. When the radius and pitch of the coil decrease, the difference

TABLE 3. Main parameters for Case 2.

Number of layers	Total number of turns	Helical	Symmetric
1	5	L1	D1
2	10	L2	D2
3	15	L3	D3
4	20	L4	D4
5	25	L5	D5

TABLE 4. Data comparison.

Pitch	Radius	3-D helical Magnetic flux	Symmetric Magnetic flux
0.5mm	8mm	4.28T	4.20T
	10mm	4.08T	3.95T
1.0mm	8mm	3.97T	3.89T
	10mm	3.79T	3.68T
1.5mm	8mm	3.79T	3.67T
	10mm	3.59T	3.48T

in magnetic flux density between the 3-D helical coil model and the symmetric coil will increase, and the error will also increase. Therefore, the effect of the solenoid coil on the pitch effect must be considered when calculating the magnetic field.

D. DISCUSSIONS

In fact, it can be drew a conclusion from the above analysis that the pitch effect of the helical coil will cause some deviations. However, from the previous analysis reveals when the number of layers of solenoid coils in the study of EMF is small, the flux density deviation calculated by the two models will decrease. Therefore, the pitch effect of the solenoid coil can be ignored, and then the solenoid coil can be directly solved as a 3-D axisymmetric model (or as a 2-D axisymmetric model). On the contrary, when the number of layers of solenoid coils is large, the flux density deviation calculated by the two models will increase, when the radius and pitch of the coil decrease, the flux density deviation calculated by the two models will increase too, so the influence of solenoid coil's pitch effect on the magnetic field calculation must be considered.

Moreover, the coils used in EMF are generally only a few layers, so it can be considered that the effect of the pitch effect of the helical coil on the forming effect of the workpiece in EMF can be ignored. Besides, the current experiments and simulations studies of EMF have also confirmed that, after the helical coil is equivalent to 2-D or3-D axial symmetry, the pitch effect of the helical coil has little influence on the forming of the workpiece, which can completely meet the actual engineering requirements [29], [31], [32].

V. CONCLUSION

To sum up, when the number of layers of the solenoid coil is small, the influence of the pitch effect can be ignored due to the small deviation, and it can be directly equivalent to the 3-D axisymmetric model for magnetic field calculation.

When the number of layers of the solenoid coil is large and the radius and pitch of the coil decrease, the influence of the pitch effect must be considered because of the large deviation.

Thereby, in the study of EMF, when the number of layers, radius and pitch used in the coil is small, the magnetic field calculation of the 3-D equivalent model is reliable. On the contrary, when the number of layers, radius and pitch used in the coil is large, the calculation deviation of the equivalent model will not accurately predict the simulation result.

REFERENCES

[1] W. Hua, X. Zhu, and Z. Wu, "Influence of coil pitch and stator-slot/rotor-pole combination on back EMF harmonics in flux-reversal permanent magnet machines," *IEEE Trans. Energy Convers.*, vol. 33, no. 3, pp. 1330–1341, Sep. 2018.

[2] J. Jinbo *et al.*, "Inductance calculation of conical winding Tesla transformer based on finite element method," *Int. J. Appl. Electromagn. Mech.*, vol. 62, no. 4, pp. 663–671, 2020.

[3] Z. Li, X. Xiang, T. Hu, A. Abu-Siada, Z. Li, and Y. Xu, "An improved digital integral algorithm to enhance the measurement accuracy of rogowski coil-based electronic transformers," *Int. J. Electr. Power Energy Syst.*, vol. 118, Jun. 2020, Art. no. 105806.

[4] Y. Cheng, G. Wang, and M. Ghovanloo, "Analytical modeling and optimization of small solenoid coils for millimeter-sized biomedical implants," *IEEE Trans. Microw. Theory Techn.*, vol. 65, no. 3, pp. 1024–1035, Mar. 2017.

[5] H. Singh, M. Ichiyanagi, and T. Suzuki, "Influence of coil pitch on thermo-fluid characteristics for square channel spiral coil sub-cooled condenser," *Int. J. Automot. Eng.*, vol. 10, no. 3, pp. 266–273, 2019.

[6] R. Prattipati, N. Koganti, and S. Pendyala, "Factors influencing hydrodynamic entry length in helical coils," in *Proc. Int. Conf. Emerg. Trends Eng.* Cham, Switzerland: Springer, 2020, pp. 616–623.

[7] Q. Xiong, H. Huang, C. Deng, L. Li, L. Qiu, and H. Tang, "A method to improve forming accuracy in electromagnetic forming of sheet metal," *Int. J. Appl. Electromagn. Mech.*, vol. 57, no. 3, pp. 367–375, Jun. 2018.

[8] X. Zhang, Q. Cao, X. Han, Q. Chen, Z. Lai, Q. Xiong, F. Deng, and L. Li, "Application of triple-coil system for improving deformation depth of tube in electromagnetic forming," *IEEE Trans. Appl. Supercond.*, vol. 26, no. 4, Jun. 2016, Art. no. 3701204.

[9] Z. Wu, Q. Cao, J. Fu, Z. Li, Y. Wan, Q. Chen, L. Li, and X. Han, "An inner-field uniform pressure actuator with high performance and its application to titanium bipolar plate forming," *Int. J. Mach. Tools Manuf.*, vol. 155, Aug. 2020, Art. no. 103570.

[10] V. Psyk, D. Risch, and B. L. Kinsey, "Electromagnetic forming-a review," *J. Mater. Process. Technol.*, vol. 211, no. 5, pp. 787–829, 2011.

[11] X. Qi, T. Hongtao, and W. Muxue, "Research progress of electromagnetic forming technique since 2011," *High Voltage Eng.*, vol. 45, no. 4, pp. 1171–1181, 2019.

[12] Q. Xiong, H. Huang, L. Xia, H. Tang, and L. Qiu, "A research based on advance dual-coil electromagnetic forming method on flanging of small-size tubes," *Int. J. Adv. Manuf. Technol.*, vol. 102, nos. 9–12, pp. 4087–4094, Jun. 2019.

[13] L. Qiu, N. Yi, A. Abu-Siada, J. Tian, Y. Fan, K. Deng, Q. Xiong, and J. Jiang, "Electromagnetic force distribution and forming performance in electromagnetic forming with discretely driven rings," *IEEE Access*, vol. 8, pp. 16166–16173, 2020.

[14] S. Ouyang, X. Li, C. Li, L. Du, T. Peng, X. Han, L. Li, Z. Lai, and Q. Cao, "Investigation of the electromagnetic attractive forming utilizing a dual-coil system for tube bulging," *J. Manuf. Processes*, vol. 49, pp. 102–115, Jan. 2020.

[15] A. Shrivastava, "Experimental and numerical study on the influence of process parameters in electromagnetic compression of AA6061 tube," *Mater. Manuf. Processes*, vol. 34, no. 13, pp. 1537–1548, 2019, doi: 10.1080/.10426914.2019.1655156.

[16] H. Yu, Q. Zheng, S. Wang, and Y. Wang, "The deformation mechanism of circular hole flanging by magnetic pulse forming," *J. Mater. Process. Technol.*, vol. 257, pp. 54–64, Jul. 2018.

[17] Q. Cao, L. Du, Z. Li, Z. Lai, Z. Li, M. Chen, X. Li, S. Xu, Q. Chen, X. Han, and L. Li, "Investigation of the Lorentz-force-driven sheet metal stamping process for cylindrical cup forming," *J. Mater. Process. Technol.*, vol. 271, pp. 532–541, Sep. 2019.

[18] E. Paese, M. Geier, R. P. Homrich, P. Rosa, and R. Rossi, "Sheet metal electromagnetic forming using a flat spiral coil: Experiments, modeling, and validation," *J. Mater. Process. Technol.*, vol. 263, pp. 408–422, Jan. 2019.

[19] Q. Xiong, H. Tang, C. Deng, L. Li, and L. Qiu, "Electromagnetic attraction-based bulge forming in small tubes: Fundamentals and simulations," *IEEE Trans. Appl. Supercond.*, vol. 28, no. 3, Apr. 2018, Art. no. 0600505.

[20] Q. Cao, Z. Li, Z. Lai, Z. Li, X. Han, and L. Li, "Analysis of the effect of an electrically conductive die on electromagnetic sheet metal forming process using the finite element-circuit coupled method," *Int. J. Adv. Manuf. Technol.*, vol. 101, nos. 1–4, pp. 549–563, Mar. 2019.

[21] H. Yu and H. Dang, "Interfacial microstructure of stainless steel/aluminum alloy tube lap joints fabricated via magnetic pulse welding," *J. Mater. Process. Technol.*, vol. 250, pp. 297–303, Dec. 2017.

[22] J. Lueg-Althoff, J. Bellmann, M. Hahn, S. Schulze, S. Gies, A. E. Tekkaya, and E. Beyer, "Joining dissimilar thin-walled tubes by magnetic pulse welding," *J. Mater. Process. Technol.*, vol. 279, May 2020, Art. no. 116562.

[23] A. Long, M. Wan, W. Wang, X. Wu, and X. Cui, "Research on controllability of final macroscopic specimen shape in electromagnetic superposed forming," *Int. J. Adv. Manuf. Technol.*, vol. 94, nos. 5–8, pp. 2679–2688, Feb. 2018.

[24] W. Liu, X. Zou, S. Huang, and Y. Lei, "Electromagnetic-assisted calibration for surface part of aluminum alloy with a dedicated uniform pressure coil," *Int. J. Adv. Manuf. Technol.*, vol. 100, nos. 1–4, pp. 721–727, Jan. 2019.

[25] W. Xiao, L. Huang, J. Li, H. Su, F. Feng, and F. Ma, "Investigation of springback during electromagnetic-assisted bending of aluminium alloy sheet," *Int. J. Adv. Manuf. Technol.*, vol. 105, nos. 1–4, pp. 375–394, Nov. 2019.

[26] L. Qiu, W. Zhang, A. Abu-Siada, G. Liu, C. Wang, Y. Wang, B. Wang, Y. Li, and Y. Yu, "Analysis of electromagnetic force and formability of tube electromagnetic bulging based on convex coil," *IEEE Access*, vol. 8, pp. 33215–33222, 2020.

[27] Q. Xiong, "A dual-coil method for electromagnetic attraction forming of sheet metals," *IEEE Access*, vol. 8, pp. 92708–92717, 2020.

[28] L. Qiu, W. Zhang, A. Abu-Siada, Q. Xiong, C. Wang, Y. Xiao, B. Wang, Y. Li, J. Jiang, and Q. Cao, "Electromagnetic force distribution and wall thickness reduction of three-coil electromagnetic tube bulging with axial compression," *IEEE Access*, vol. 8, pp. 21665–21675, 2020.

[29] Q. Cao, L. Li, Z. Lai, Z. Zhou, Q. Xiong, X. Zhang, and X. Han, "Dynamic analysis of electromagnetic sheet metal forming process using finite element method," *Int. J. Adv. Manuf. Technol.*, vol. 74, nos. 1–4, pp. 361–368, 2014.

[30] B. Zhu, Q. Zeng, Y. Chen, Y. Zhao, and S. Liu, "A dual-input high step-up DC/DC converter with ZVT auxiliary circuit," *IEEE Trans. Energy Convers.*, vol. 34, no. 1, pp. 161–169, Mar. 2019.

[31] X. Li, Q. Cao, Z. Lai, S. Ouyang, N. Liu, M. Li, X. Han, and L. Li, "Bulging behavior of metallic tubes during the electromagnetic forming process in the presence of a background magnetic field," *J. Mater. Process. Technol.*, vol. 276, Feb. 2020, Art. no. 116411.

[32] Q. Xiong, H. Tang, M. Wang, H. Huang, L. Qiu, K. Yu, and Q. Chen, "Design and implementation of tube bulging by an attractive electromagnetic force," *J. Mater. Process. Technol.*, vol. 273, Nov. 2019, Art. no. 116240.

WENTING ZHANG received the M.S. degree in electrical engineering from China Three Gorges University, Yichang, China, in 2014.

She is currently a Lecturer with the College of Electrical Engineering and New Energy, China Three Gorges University. Her research interests include technology of pulsed high-magnetic field, high-voltage technology, and electromagnetic forming.

HANG ZHOU is currently pursuing the bachelor's degree in electrical engineering and automation with the College of Electrical Engineering and New Energy, China Three Gorges University, Yichang.

XIAOGUANG LIANG is currently a Senior Engineer with the Beijing Institute of Aerospace Systems Engineering. His research interest includes design of liquid carrier rocket propellant tank structure.

XIANQI SONG is currently pursuing the degree in electrical engineering with the College of Electrical Engineering and New Energy, China Three Gorges University, Yichang.

LIJUN ZHOU is currently pursuing the degree in electrical engineering with the College of Electrical Engineering and New Energy, China Three Gorges University, Yichang.

SHUIXIANG LI is currently a Senior Engineer with Central China Normal University. His research interests include instrument and testing technology.

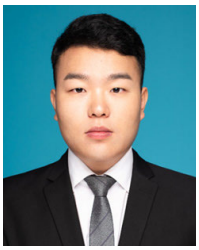

MENG YANG is currently pursuing the degree in electrical engineering with the College of Electrical Engineering and New Energy, China Three Gorges University, Yichang. His research interests include technology of pulsed high-magnetic field, high-voltage technology, and electromagnetic forming.

XINHUI ZHU is currently pursuing the degree in electrical engineering with the College of Electrical Engineering and New Energy, China Three Gorges University, Yichang. His research interests include technology of pulsed high-magnetic field, high-voltage technology, and electromagnetic forming.